Bonding in hard and elastic amorphous carbon nitride films investigated using ^{15}N, ^{13}C, and ^{1}H NMR spectroscopy

W. J. Gammon,[1] G. L. Hoatson,[1] B. C. Holloway,[2] R. L. Vold,[2] and A. C. Reilly[1]
[1]*Department of Physics, College of William & Mary, P.O. Box 8795, Williamsburg, Virginia 23187, USA*
[2]*Department of Applied Science, College of William & Mary, P.O. Box 8795, Williamsburg, Virginia 23187, USA*
(Received 14 February 2003; published 5 November 2003)

The nitrogen bonding in hard and elastic amorphous carbon nitride (a-CN_x) films is examined with ^{15}N, ^{13}C, and ^{1}H nuclear magnetic resonance (NMR) spectroscopy. Films were deposited by dc magnetron sputtering, in a pure nitrogen discharge on Si(001) substrates at 300 °C. Nanoindentation tests revealed an elastic recovery of 80%, a hardness of 5 GPa, and an elastic modulus of 47 GPa. The NMR results show that nitrogen bonding in this material is consistent with sp^2 hybridized nitrogen incorporated in an aromatic carbon environment. The data also indicate that the a-CN_x prepared for this study has very low hydrogen content and is hydrophilic. Specifically, analysis of ^{15}N and ^{13}C cross polarization magic angle spinning and ^{1}H NMR experiments suggests that water preferentially protonates nitrogen sites.

DOI: 10.1103/PhysRevB.68.195401 PACS number(s): 81.05.Tp, 81.15.Cd, 62.20.−x, 76.60.−k

INTRODUCTION

Incorporating nitrogen into carbon films can improve their mechanical properties. When deposited under suitable conditions, amorphous carbon nitride (a-CN_x) films are fabricated with low elastic modulus but with high strength and high elastic recovery.[1,2] Early work on a-CN_x proposed that a turbostratic structure consisting of cross-linked buckled graphitic layers accounts for its strength and high elasticity.[3] A current research focus is to identify unknown structures responsible for bending and cross linking the graphitic layers. However, the identity of these structures and nitrogen bonding in a-CN_x remain unknown.

Many publications have been devoted to the study of nitrogen bonding in a-CN_x films. In particular, x-ray photoelectron spectroscopy (XPS)[1,2,4–6] and vibrational spectroscopy[7-11] measurements have been the most common techniques used to investigate this subject. However, interpretation of these data varies widely in the literature. This is not surprising, since the varieties of different bonding configurations are too close in energy. Thus, one is faced with interpreting spectra with a multitude of overlapping peaks, which makes deconvolution problematic.

In this study, solid-state nuclear magnetic resonance (NMR) spectroscopy is used to elucidate the chemical bonding in a-CN_x. The advantage of NMR is its high sensitivity to the electronic environment, which is reflected in the isotropic chemical shift. NMR chemical shifts are more sensitive than XPS values, and thus provide a better description of bonding. Taking advantage of this greater sensitivity, plausible chemical shift assignments are made, and the bonding configurations that play dominant roles in a-CN_x are determined.

Unfortunately, NMR has an inherent disadvantage in that a large amount of material ($\sim$100 mg) is required to make measurements—a requirement that is difficult to fulfill using film fabrication techniques. This presumably explains the limited attention NMR has received from the carbon nitride community. The few researchers who used NMR to investigate a-CN_x films have focused on hydrogenated materials or materials deposited at ambient temperature.[12-15] However, a-CN_x materials deposited under these conditions have less robust mechanical properties.[16,17] Mechanical testing results were not reported for the materials previously characterized by NMR,[12-15] and it is doubtful if those were the highly elastic and mechanically hard material of interest.

In this study, our materials have been characterized by ^{15}N, ^{13}C, and ^{1}H NMR measurements in addition to nanoindentation. The primary focus of this report is on the ^{15}N NMR results, which elucidate the nature of nitrogen bonding in a-CN_x. These results complement our previous ^{13}C NMR study.[18] In addition, results from ^{15}N cross polarization (CP) and ^{1}H magic angle spinning (MAS) NMR experiments suggest that nitrogen sites are susceptible to protonation from water absorbed during sample preparation for the NMR measurements. This result may be contrasted with our previous report,[18] where we showed that the overall fraction of protonated carbons in our material is very low. Specifically, our results indicate that nitrogen sites are more susceptible to protonation than carbon sites. In an attempt to clarify this result, we have compared the contact time dependence of the ^{13}C CPMAS spectra with our previous REAPDOR measurements.[18] This comparison indicates that those carbons that are protonated are also more likely to be directly bonded to nitrogen. Finally, we present a film-structure model for hard and elastic a-CN_x, which is based on the insights provided by the ^{15}N NMR results as well as those from our previous ^{13}C NMR study.[18]

EXPERIMENTAL

The a-CN_x films were deposited by dc magnetron sputtering in a pure nitrogen discharge at 1.2 Pa on 75 mm diam. Si(001) substrates, using a 50-mm, sputtering gun (Mighty-Mak U.S. Inc.). The target was a 99.999% pure graphite disk with 50 mm diameter and 6.4 mm thickness. The sample was mounted on a radiatively heated substrate holder, which was positioned 8 cm from the target face. During film deposition,

the substrate was electrically grounded and heated to 300 °C, and the target discharge current was limited to 300 mA. The ultimate pressure of the vacuum system was 3×10^{-5} Pa at room temperature. An $^{15}N_2$ and $^{14}N_2$ feedstock gas mixture was used to enrich the material fabricated for the ^{15}N NMR measurements. The total gas-flow was regulated by a precision gas-flow controller at 10 sccm with flow rates set at 4 and 6 sccm for the $^{15}N_2$ and $^{14}N_2$ gases, respectively. However, for the ^{13}C and ^{1}H measurements, experiments were carried out on the unenriched a-CN_x sample used in our previous NMR study.[18] The deposition rate of the material was determined to be ~1 μm/h, as determined by a thickness profile measurement using scanning electron microscopy.

For the NMR measurements, 180 mg of material was prepared by depositing four, 8 μm-thick films. The material was scraped off the substrates, ground to a fine powder using a mortar and pestle, and packed into a 5 mm zirconia rotor. All solid-state NMR measurements were made with a custom-built spectrometer operating at 7 T (^{1}H Larmor frequency of 300.07 MHz) with a ^{13}C frequency of 75.46 MHz and an ^{15}N frequency of 30.41 MHz. The 90° pulse widths for the ^{1}H, ^{13}C, and ^{15}N detection experiments were 5, 4, and 4 μs, respectively. For proton decoupling, a radio frequency field-strength of 71.4 kHz was used for proton decoupling.

Magic angle spinning (MAS) ($\nu_r=8-9$ kHz) NMR direct-detection and cross polarization (CP) spectra were obtained using a Hahn-echo pulse sequence $(90_x-\tau_e-180_x)$ for the ^{15}N and ^{13}C measurements, and a solid-echo sequence $(90_x-\tau_e-90_y)$ for the ^{1}H experiments. Comparison between spectra collected by direct detection versus cross polarization provided valuable insight into the extent of hydrogen bonding in the material.[18] The cross polarization experiments are double resonance techniques in which the signal is obtained by the transfer of spin polarization from protons to the detected spins (here, ^{13}C or ^{15}N). Since in spin polarization transfer from ^{1}H to the detected spins is mediated by the strength of the dipolar coupling (and therefore inter-nuclear distances),[19] the proton connectivity associated with particular carbons[18] or nitrogens in the spectrum can be inferred. Specifically, sites with associated with directly bonded protons can be readily discerned from those with remotely coupled protons.

Cross polarization with population inversion (CPPI)[20] was used to provide partial spectral editing of the ^{15}N spectra. All NMR spectra were obtained at room temperature except for the ^{1}H spectra, which were obtained at both room temperature and 150 °C. For the ^{1}H NMR experiments at high temperature, the sample was first heated for 20 min at 150 °C, and then data were acquired at 150 °C for an additional 22 min. Additional experimental details of recycle delays (τ_d), echo spacing times (τ_e), spinning speeds (ν_r), number of scans (NS), and apodization by Lorentzian line broadening (LB) are included in the figure captions. The reported ^{15}N chemical shifts are referenced to labeled glycine at -348 ppm on the nitromethane scale (CH_3NO_2 at zero ppm), and the ^{13}C chemical shifts are referenced to the carboxyl carbon of glycine at 176 ppm on the tetramethylsilane scale (TMS at zero ppm). The ^{1}H chemical shifts are referenced to water at 5.3 ppm (TMS at zero ppm).

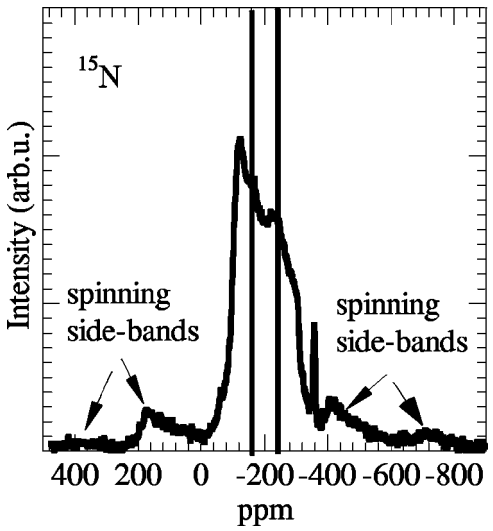

FIG. 1. ^{15}N Hahn-echo MAS spectrum with proton decoupling ($\tau_d=30$ s, $\tau_e=111.1$ μs, $\nu_r=9$ kHz, NS=11 160 transients, and no apodization). The shape of the spectrum suggests at least five bonding configurations at the following estimated positions: -120, -160, -255, -295, and -358 ppm. The vertical lines indicate the calculated chemical shift of the two nitrogen-sites in graphitic C_3N_4 (Ref. 23).

RESULTS

The mechanical properties of this material have been reported in an earlier publication.[18] To summarize, nanoindentation tests gave a hardness of 5 GPa and an elastic modulus of 47 GPa for an indentation depth of 100 nm, as obtained by the method of Oliver and Pharr.[21] The a-CN_x films exhibit a high elastic recovery of 80% at 1.0 mN maximum load. We also demonstrated that the mechanical properties are uniform across the entire diameter of the 75 mm substrate,[18] which proves the integrity of our deposition method for producing the large quantity of material needed for the NMR experiments.

The direct-detection ^{15}N MAS spectrum (Fig. 1) was obtained with 11 160 scans using a 30 s recycle delay. By comparing spectra obtained at 20 and 30 s recycle delays, the spin-lattice relaxation time was estimated: $T_{1z}\sim15$ s. The broad, low- intensity features positioned symmetrically around the central portion of the spectrum are spinning side bands (296 ppm=9 kHz).

Hahn-echo ^{15}N MAS spectra obtained using direct detection and cross polarization experiments are compared in Fig. 2. The direct-detection spectra obtained with (solid line) and without (dotted line) proton decoupling are indicated in the top traces; proton decoupling has the greatest affect on the intensity of the broad shoulder in the range between -210 to -330 ppm. Without proton decoupling, the spectral feature centered approximately at -295 ppm (top traces) is notably dephased. For comparison, a CP spectrum obtained using a 1 ms contact time (dashed line in lower portion of Fig. 2) is

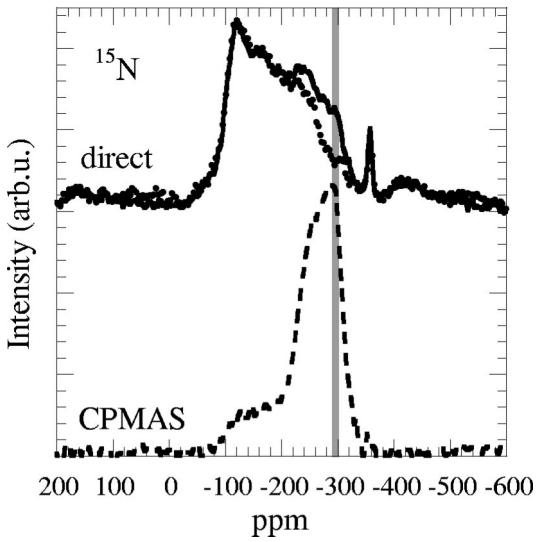

FIG. 2. ^{15}N Hahn-echo MAS spectra obtained by direct-detection and cross polarization experiments. The direct-detection spectra ($\tau_d = 30$ s, $\tau_e = 111.1\ \mu$s, $\nu_r = 9$ kHz, NS = 2480, and LB = 50 Hz) obtained with and without proton decoupling are indicated by the solid line and dotted line, respectively. A CPMAS spectrum with 1 ms contact time ($\tau_d = 1$ s, $\tau_e = 111.1\ \mu$s, $\nu_r = 9$ kHz, NS = 2480, and LB = 50 Hz) is displayed at the bottom (dashed line) for comparison. The spectral feature near -295 ppm (gray line) is markedly dephased in absence of proton decoupling, and this feature coincides with the highest cross polarization efficiency.

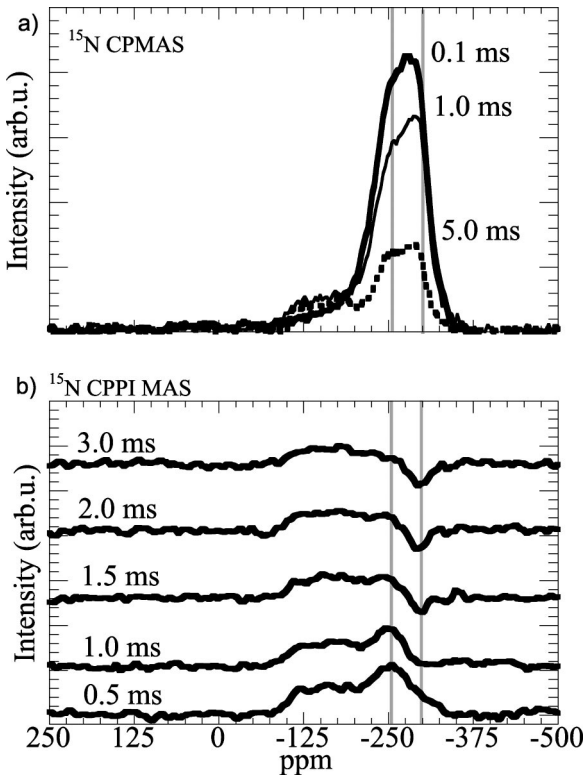

FIG. 3. (a) ^{15}N CPMAS spectra ($\tau_d = 1$ s, $\tau_e = 111.1\ \mu$s, $\nu_r = 9$ kHz, NS = 2480, and LB = 50 Hz) obtained at 0.1, 1.0, and 5 ms contact times. The efficient cross polarization of the feature centered at -275 ppm at short contact times indicates that this nitrogen bonding site is protonated. (b) ^{15}N CPPI MAS spectra ($\tau_d = 1$ s, $\tau_e = 111.1\ \mu$s, $\nu_r = 9$ kHz, NS = 600, and LB = 200 Hz) for various PI times ranging from 0.5 to 3.0 ms following an initial 1 ms contact time. Peak positions estimated from the CPPI measurement are indicated by the gray lines at -295 and -255 ppm.

also displayed. Notice that the highest cross polarization efficiency is observed at -295 ppm (gray line), precisely where the direct detection spectrum exhibits the largest dephasing with out proton decoupling. This is to be expected since in the absence of decoupling the ^{15}N and ^{1}H will be dipolar coupled.

CPMAS ^{15}N spectra obtained at 0.1, 1.0, and 5.0 ms contact times are shown in Fig. 3(a). Evolution of the ^{15}N CPMAS spectra with contact time suggests at least two ^{15}N-^{1}H dipolar coupling strengths for polarization transfer. Cross polarization is very effective at short contact times (0.1 ms) for the high intensity feature centered near -275 ppm, indicating dipolar coupling to directly bonded protons. However, cross polarization is not efficient for the low-intensity broad shoulder centered near -160 ppm. The intensity of this shoulder increases up to 1 ms contact time, and remains constant out to at least 5 ms. The low relative intensity and slow build-up of the polarization indicates that these nitrogens have no directly bonded protons, which is consistent with the behavior shown in Fig. 2; the portion of the direct-detection spectra near -160 ppm is insensitive to the dipolar dephasing time period.

The shape of the peak centered near -275 ppm [Fig. 3(a)] suggests at least two nitrogen bonding configurations. To distinguish these, CPPI measurements were performed using a 1 ms initial contact time, as shown in Fig. 3(b). As indicated by the gray vertical lines in the CPPI spectra, the high-intensity feature in the CPMAS spectrum is composed of two nitrogen bonding types, which are centered at approximately -255 and -295 ppm. The inversion time for the peak at -295 ppm occurs between 0.5 and 1.0 ms PI times, while the other portions of the spectrum retain a positive intensity for PI times greater than 3.0 ms.

MAS ^{13}C NMR spectra of a-CN_x as obtained by rotational-echo, adiabatic-passage, double-resonance (REAPDOR), and Hahn-echo CPMAS are compared in Fig. 4. The results from the REAPDOR experiment (upper traces) were published in our previous ^{13}C NMR study;[18] the full spectrum (filled squares) is compared to the attenuated spectrum (open circles). The attenuated spectrum is obtained by applying a dipolar dephasing pulse to the ^{14}N channel.[22] Since the strength of the dipolar interaction is inversely proportional to the cube of the internuclear bond distance, those ^{13}C bonded closest to ^{14}N experience the strongest dipolar dephasing. Thus the highest dephasing efficiency (signal attenuation) is observed for carbons directly bonded to nitrogen. The gray shaded region indicates the portion of the ^{13}C spectrum that is coupled to ^{14}N nuclei. The largest dephasing occurs at 150 ppm, as indicated by the solid vertical line. The REAPDOR spectra are also compared with ^{13}C CPMAS measurements (lower traces) obtained using contact times of 1 ms (dashed line) and 5 ms (solid line). Note that at short contact times (1

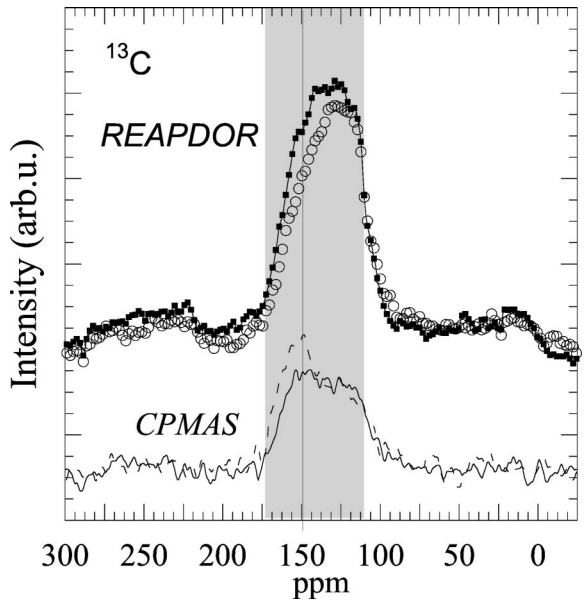

FIG. 4. REAPDOR spectra (upper traces) were acquired with $\tau_d = 3$ s; $\nu_r = 8$ kHz; and NS = 26 000. The full spectrum (filled squares) and attenuated spectrum (open circles) are shown. The gray shading indicates the region of the spectra with carbons directly bonded to nitrogen. Hahn-echo CPMAS spectra (lower traces) obtained using contact times of 1 ms (dashed line) and 5 ms (solid line) ($\tau_d = 1$ s; $\tau_e = 111.1$ μs; $\nu_r = 9$ kHz; NS = 10 000, and LB = 200 Hz).

ms), the CPMAS spectra exhibit a sharp peak at ~150 ppm, precisely where the REAPDOR spectra exhibit the largest dephasing.

The temperature dependence of the ^{1}H MAS NMR spectra of a-CN_x was also investigated, as shown in Fig. 5. The data were first collected on the as-prepared sample (solid line). Then, the sample was heated inside the probe for 20 min. at 150 °C, and this temperature was maintained during data acquisition (~22 min). The heat treatment caused a large reduction of the ^{1}H MAS spectral intensity (dashed line) and revealed a previously unresolved feature near 0 ppm.

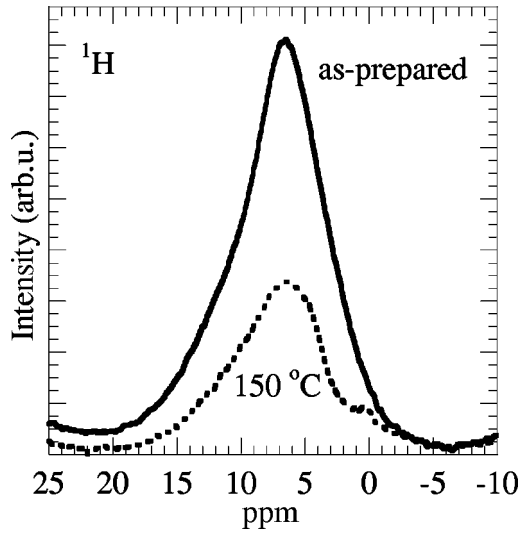

FIG. 5. Comparison of ^{1}H MAS NMR spectra ($\tau_d = 1$ s, $\tau_e = 250$ μs, $\nu_r = 8$ kHz, NS = 1320, and LB = 100 Hz) between the as-prepared material (solid line) and after heating at 150 °C (dashed line). After heating, the spectral intensity centered at 6.5 ppm is greatly reduced, which suggests desorbtion of water.

DISCUSSION

The direct-detection ^{15}N MAS spectrum with proton decoupling (Fig. 1) suggests at least five different bonding environments: these are positioned approximately at −120, −160, −255, −295, and −358 ppm. Estimates of the peak-center values near −120 and −160 ppm were obtained from the zero crossings of the first derivative spectrum. The values of −255 and −295 ppm were inferred from the CPPI measurements [shown in Fig. 3(b)], and the value of −358 ppm for the sharp feature was obtained from its point of maximum intensity. The black vertical lines (Fig. 1) indicate the calculated ^{15}N chemical shifts of the two nonequivalent sites in graphitic C_3N_4, as obtained by Yoon *et al.*[23] These two nitrogen sites are on the perimeter of a vacancy defect: a nitrogen site bonded to two carbons (similar to pyridine) at −166 ppm together with a nitrogen site bonded to three carbons (similar to a substitutional site in graphite) at −240 ppm.[23] The ^{15}N chemical shifts found in a-CN_x indicate that these bonding types may account for the features observed at −160 and −255 ppm. This suggestion is consistent with our previous ^{13}C NMR results,[18] from which we infer that a-CN_x has an sp^2 carbon bonded structure, since the spectra rule out sp^3 bonded carbons. However, we point out that their calculated ^{15}N chemical shift for pyridine is 43 ppm lower than its experimental value.[23] This suggests that the calculated value of −166 ppm for graphitic C_3N_4 is similarly shifted. Applying the same shift, the value of −166 ppm becomes −123 ppm; note that the value of −123 ppm is very close to the value for the feature at −120 ppm in a-CN_x.

We have also compared our experimental ^{15}N MAS spectra (Figs. 1 and 2) with two compilations of ^{15}N chemical shifts.[24,25] The isotropic chemical shifts listed in Ref. 24 are based on liquid state NMR measurements, while those in Ref. 25 are from solid-state measurements. In addition, Ref. 24 includes some ^{14}N chemical shift data, and these results were included in the comparison. The reference chemical shift data[24,25] are schematically summarized in Fig. 6. For clarity, pyridinelike and pyrrolelike bonding types are depicted in Fig. 7. The chemical shifts for pyridinelike and pyrrolelike nitrogens were taken exclusively from measurements on solutions,[24] and specific examples are shown in Fig. 6. For compounds with both nitrogen types (as an example see Fig. 7), only those with $R \neq H$ were considered in this comparison. Since, if $R = H$, then the chemical shift between the two sites is averaged due to affects of proton tautomerism.

The comparison in Fig. 6 suggests that the spectral feature at −120 ppm is due to nitrogen bonded in a pyridinelike or nitrile bonding configuration. However, our previous Fourier transform infrared spectroscopy work indicates that the frac-

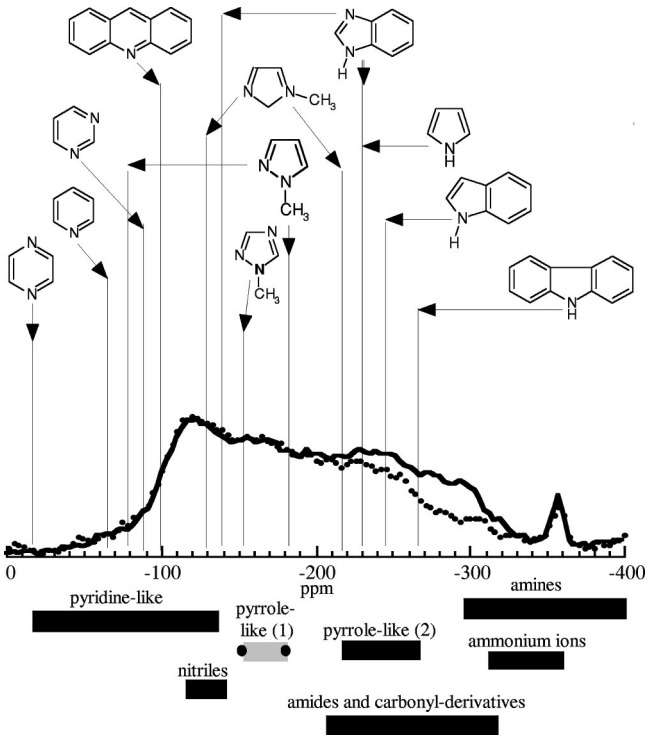

FIG. 6. A schematic display of ^{15}N isotropic NMR chemical-shift ranges for various bonding configurations (Refs. 24, 25). For ease of comparison, the ^{15}N direct-detection spectra from Fig. 2 are shown.

tion of nitrile bonds is small in our material.[2] Therefore, we assume a pyridinelike nitrogen site and do not consider nitrile bonding further.

Furthermore, the spectral features at -160 and -255 ppm are in the range of nitrogens bonded in pyrrolelike configurations (see Fig. 6). The indicated pyrrolelike range[24] is subdivided into two categories: pyrrolelike nitrogen with (1) or without (2) a directly bonded nitrogen neighbor. The available chemical-shift data for type-(1) nitrogens are very limited,[24] and thus should be considered with caution. In addition, only those type-(1) pyrrolelike nitrogens that are methylated were considered, as opposed to protonated (see above discussion on proton tautomerism). This small data set (two compounds) suggests that type-(1) nitrogens are more deshielded,[24] as schematically indicated by the

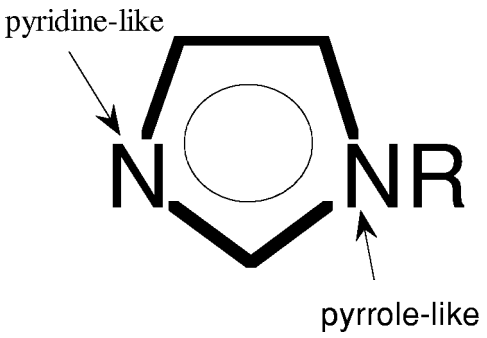

FIG. 7. Configurations of pyridinelike and pyrrolelike nitrogen (Ref. 24).

range of the gray-shaded bar shown in Fig. 6. If the gray region can completely account for this bonding contribution, then a region of equal intensity for the nitrogen neighbor that is directly bonded to the pyrrolelike N should also appear in the spectrum. These directly bonded nitrogen neighbor can be described as pyridinelike and has a chemical shift in that range (Fig. 6).[24] To settle the question of N-N bonding, future experiments that exploit homonuclear dipole-dipole coupling are planned.

Comparing literature values with our results (see Fig. 6) suggests that the features near -255 and -295 ppm might arise, in part, from nitrogen in amides or carbonyl derivatives. However, this assignment is implausible. If these features in the ^{15}N spectra are associated with an amide then a corresponding feature due to C=O should appear in the ^{13}C spectra near 168–177 ppm[25] (Fig. 4). This feature is not evident in the ^{13}C spectra (also see our previous report, Ref. 18), ruling out the presence of carbonyl groups. In addition, the spectral region covered by amines slightly overlaps with the intensity near -295 ppm. Finally, the sharp feature at -358 ppm falls in the range of amines,[24] ammonium ions,[24] or isocyanate structures.[25] Since this feature (-358 ppm) makes up a small percentage of the overall integrated intensity, it will not be discussed further. In summary, comparison to reference chemical shift data suggests that nitrogen bonding in a-CN_x is predominately sp^2 and exists in pyridinelike or pyrrolelike configurations. Unfortunately, experimental ^{15}N chemical shifts are unavailable for nitrogen coordinated to three carbons in graphene segments.

In the direct-detection ^{15}N spectra without proton decoupling (Fig. 2), the spectral feature near -295 ppm is considerably dephased, and this feature coincides with the highest intensity of the ^{15}N CPMAS spectrum. These observations show that this nitrogen site is protonated; this conclusion is further supported by the observation that the CPMAS spectra show the highest efficiency for short contact times [Fig. 3(a)]. It is important to note that the other portions of the direct-detection spectra (Fig. 2) are either unaffected or at most slightly influenced by proton decoupling. Indeed, the overall resolution of the spectra is not greatly affected by proton decoupling. These results suggest that water adsorption during NMR sample preparation is the most likely source of proton contamination. If the majority of protons had been introduced during film deposition, one would expect that the entire ^{15}N spectrum to be influenced by proton decoupling. However, we estimate an 8% relative intensity loss due to proton dipolar dephasing, which shows that only a small fraction of the nitrogens are protonated. In addition, this small change indicates that not all of the intensity near -295 ppm (direct detection spectra in Fig. 2) arises from protonated nitrogen.

If hydrogenation of the material is due to adsorbed water, the portions of the ^{15}N direct-detection spectrum (Fig. 2) that are affected by proton decoupling (region between -210 and -330 ppm) may arise from a chemical shift due to protonation by water of the less-shielded portions of the spectrum (regions between -30 and -210 ppm). For example, one possible explanation is due to protonation of pyridine-like nitrogen, which would strongly shield the nitrogen site and

yield a chemical shift of approximately 100 ppm.[24] The ^{15}N CPMAS spectra [Fig. 3(a)] exhibit two major features separated by approximately 100 ppm: a peak centered near -275 ppm and a broad shoulder centered near -160 ppm. This may indicate that the peak near -275 ppm arises from protonation of the species associated with the region near -160 ppm. The observed cross polarization behavior of these peaks [Fig. 3(a)] is consistent with this idea. The slow build-up of the CPMAS intensity in the region near -160 ppm, as a function of contact time, indicates remote, weakly coordinated protons. While, the high cross-polarization efficiency of the intense peak in the region near -275 ppm originates from protonated or hydrated species. The possibility of water absorption is currently being explored; CPMAS and direct detection intensities are being recorded as a function of temperature and time.

In our previous ^{13}C NMR study, we demonstrated that most of the carbons were unprotonated.[18] This result was supported by much lower absolute intensity of the CPMAS spectra compared to direct-detection spectra, and was supported by the fact that the direct-detection spectra are unaltered by proton decoupling.[18] In the present report, the influence of protonation in a-CN_x is further explored by comparing ^{13}C REAPDOR and variable contact time CP measurements (Fig. 4). The REAPDOR results (upper traces in Fig. 4) show the largest dipolar dephasing occurs near 150 ppm.[18] Interestingly, the CPMAS ^{13}C spectra (lower traces in Fig. 4) show that the intensity of the peak observed at 150 ppm (gray line) decreases as the contact time is lengthened from 1 ms to 5 ms. Together these results suggest that those carbons directly bonded to nitrogen are closest to protons. Moreover, these results are compatible with our observation that nitrogen sites exhibit the highest level of protonation.

Proton MAS NMR spectra, before and after annealing at 150 °C, are shown in Fig. 5. During the heating process, the integrated intensity of the proton spectra—centered at 6.5 ppm—dropped by 57%. This suggests that the spectral feature centered at 6.5 ppm is predominantly due to physisorbed water. After heating at 150 °C, the proton spectrum shows an additional small feature near 0 ppm. The origin of this small peak may be due to protons bonded to something less electronegative than oxygen, which is indicative of protons directly bonded to nitrogen sites in a-CN_x. This is plausible, since results from our previous ^{13}C study spectra on hard and elastic a-CN_x indicate that the carbons are not significantly hydrogenated.[18] Alternatively, this small feature may be due, in part, to hydroxyl species.

Previous computational work by Johansson and Stafström[26] suggested a bonding model for a-CN_x that incorporates sp^3 carbons to explain the hardness of the material. However, our previous ^{13}C NMR study demonstrated the absence of sp^3 carbons.[18] Their model is thus inconsistent with our result. Furthermore, Johansson and Stafström proposed that the nitrogen bonded to sp^3 carbons are in a tertiary amine configuration, as in the model structure $N[C(CH_3)_3]_3$. However, our ^{15}N results indicate that the amount of amine present is small (see comparison depicted in Fig. 6). Our work demonstrates that Johansson and Stafström's bonding model[26] is not applicable to hard and elastic a-CN_x. Collectively, our NMR and nanoindentation results imply that our a-CN_x material has an aromatic carbon structure with nitrogen bonded in heterocyclic rings.

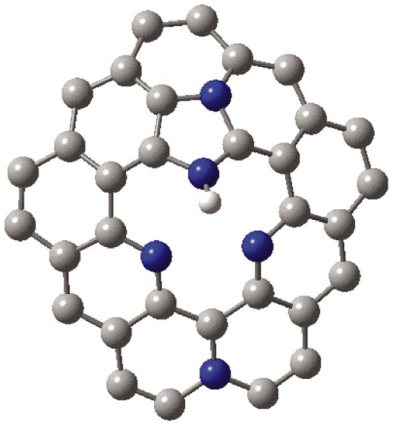

FIG. 8. (Color) A proposed film-structure model for a-CN_x. The gray shaded spheres are carbon atoms and the blue spheres are nitrogen atoms. The white sphere is a hydrogen atom, which is bonded to the nitrogen at the pentagon-vertex on the perimeter of the vacancy.

The calculated ^{15}N and ^{13}C chemical shifts[23] of graphitic C_3N_4 are coincident with the range covered by our experimental spectra (Figs. 1 and 4), which suggests that N bonding at the perimeter of vacancy defects, as found in graphitic C_3N_4, may also occur in a-CN_x. Computational work by Snis and Matar[27] on the model compound $C_{11}N_4$ demonstrates an XPS N($1s$) chemical shift of ~ 2 eV between the two types of nitrogen sites on the perimeter of a single-atom vacancy in a graphitic layer: a site with nitrogen coordinated to two carbons and a site with nitrogen coordinated to three carbons. Their prediction is consistent with the experimental XPS chemical shift of the two main N($1s$) bonding components observed in the spectra of hard and elastic a-CN_x.[1,2,4–6] Thus, NMR and XPS data are compatible with the proposal that vacancy defects in graphitic layers occur in a-CN_x films.

Previous transmission electron microscopy work indicates that hard and elastic a-CN_x consists of buckled graphitic planes that are cross linked together.[3] Furthermore, our experimental data suggest that nitrogen bonded in a pyrrolelike configuration is present in the material (Fig. 6). Incorporation of five-membered rings in the material, similar to pyrrole, would allow the graphitic planes to buckle. Thus, we propose a model that incorporates vacancy defects and pentagons; a schematic of one such model is shown in Fig. 8. This film-structure model allows for the incorporation of pyridinelike nitrogen and for the buckling of graphitic planes. We propose that cross linking occurs at dangling bond (twofold coordinated) sites on the perimeter of a vacancy. In particular, a pentagon placed next to a single-atom vacancy in a graphitic layer will have a twofold coordinated vertex; such a site is anticipated to be very reactive due to high curvature.

CONCLUSIONS

The ^{13}C and ^{15}N chemical shifts observed in direct-detection NMR spectra were compared with the calculated

chemical shifts of a variety of C_3N_4 structures[23] and with tabulated compilations of experimental ^{15}N chemical shifts from various organic molecules.[24,25] Only the calculated ^{13}C chemical shift of graphitic C_3N_4 (144 ppm) falls in the range of our experimental spectra. The graphitic phase of C_3N_4 has two nonequivalent nitrogen sites on the perimeter of a single-atom vacancy. The calculated ^{15}N chemical shifts are -240 ppm for the site coordinated to three sp^2 carbons and -166 ppm for the site coordinated to two sp^2 carbons (pyridinelike site).[23] These values are in close agreement with the observed ^{15}N peak positions at -160 and -255 ppm. However, experimental ^{15}N chemical shift values for nitrogen that are threefold coordinated in a graphene sheet are unavailable, and other computational values are unavailable to compare with the feature at -240 ppm in graphitic C_3N_4. Moreover, literature reports[2,28] indicate that the N/C ratios are typically less than <0.33 for amorphous carbon nitride (a-CN_x) fabricated by dc magnetron sputtering. This is clearly less than the N/C ratio found in graphitic C_3N_4. Nevertheless, similarities in bonding between the two materials may exist.

Further comparison of our data with tabulated ^{15}N chemical shift values (Fig. 6) suggest that the spectral feature near -120 ppm is due to pyridine-like nitrogen; this is similar to the ^{15}N assignment of the calculated chemical shift near -166 ppm in graphitic C_3N_4. In addition, this same comparison suggests an assignment of nitrogen bonded in a pyrrolelike configuration for the features at -160 and -255 ppm. Cross polarization magic angle spinning (CPMAS) ^{15}N experiments suggest that portions of the feature near -295 ppm are protonated. However, it is unlikely that this feature is due to protonated nitrogens that are bonded adjacent to a carbonyl group, since carbonyl ^{13}C chemical shifts typically fall in the range of 168–177 ppm[25] and are unobserved in our ^{13}C spectra (see Fig. 4 as well as results in Ref. 18).

As shown in our previous report,[18] proton decoupling had a negligible effect on the direct-detection ^{13}C spectra. Thus, it can be inferred that the majority of carbons in our a-CN_x are not directly bonded to protons. This is further supported by the low efficiency of ^{13}C CPMAS experiments. However in the ^{15}N direct-detection spectra, proton decoupling has a notable influence on the spectral feature at -295 ppm. In particular, the dephasing and high cross polarization efficiency at short contact times indicate that nitrogens corresponding to portions of the spectrum near -295 ppm have protons in close proximity. The most likely proton source in a-CN_x is adsorbed water. This conjecture is supported by ^1H NMR experiments, which indicate water desorbtion during sample heating. These results indicate that certain nitrogen bonding sites are hydrophilic, and are protonated by physisorbed water. In particular, we suggest that portions of the ^{15}N direct-detection spectrum that are affected by proton decoupling may arise from a chemical shift due to protonation by water of the less-shielded portions of the spectrum.

These multinuclear NMR results confirm our conclusions that the structure of a-CN_x lacks sp^3 carbons[18] and that the interconnecting structure is not hydrogen bonded. Considering our NMR and nanoindentation results from the same a-CN_x material, the most consistent bonding model is an aromatic carbon structure with nitrogen bonded in heterocyclic rings. The similarity of the ^{15}N chemical shifts in graphitic C_3N_4 and in hard and elastic a-CN_x suggests that the same single-atom vacancy defects may occur in a-CN_x. This is consistent with the calculated x-ray photoelectron spectroscopy (XPS) chemical shifts of $C_{11}N_4$, which has a vacancy defect structure.[27] Our experimental ^{15}N data are also consistent with nitrogen bonded in a pyrrolelike configuration. Thus, we propose a film-structure model that incorporates nitrogen bonding on the perimeter of vacancy defect structures and pentagons. Pentagon incorporation would account for the buckled graphitic layers observed by transmission electron microscopy.[3,28]

ACKNOWLEDGMENTS

The authors thank O. Kraft for the nanoindentation measurements and D.I. Malyarenko for her invaluable assistance and guidance with the NMR experiments. This work was supported by the Jeffress Memorial trust (J-504), the NSF under Grant No. CHE-0079316 (G.L.H. and R.L.V.), the Research Corporation under Grant No. RI0449 (A.C.R.), the American Chemical Society Petroleum Research Fund under Grant No. ACS-PRF 36597-65 (A.C.R.), and the office of Naval Research under Grant No. N00014-02-1-0711 (B.C.H.)

[1] W. J. Gammon, O. Kraft, A. C. Reilly, and B. C. Holloway, Carbon **41**, 1917 (2003).
[2] B. C. Holloway, O. Kraft, D. K. Shuh, W. D. Nix, M. Kelly, P. Pianetta, and S. Hagstrom, J. Vac. Sci. Technol. A **18**, 2964 (2000).
[3] H. Sjöström, S. Stafström, M. Boman, and J.-E. Sundgren, Phys. Rev. Lett. **75**, 1336 (1995).
[4] D. Marton, K. J. Boyd, A. H. Al-Bayati, S. S. Todorov, and J. W. Rabalais, Phys. Rev. Lett. **73**, 118 (1994).
[5] C. Ronning, H. Feldermann, R. Merk, H. Hofsass, P. Reinke, and J. U. Thiele, Phys. Rev. B **58**, 2207 (1998).
[6] C. Spaeth, M. Kuhn, F. Richter, U. Falke, M. Hietschold, R. Kilper, and U. Kreissig, Diamond Relat. Mater. **7**, 1727 (1998).
[7] J. H. Kaufman, S. Metin, and D. D. Saperstein, Phys. Rev. B **39**, 13 053 (1989).
[8] A. Chowdhury, D. C. Cameron, and M. S. J. Hashmi, Thin Solid Films **332**, 62 (1998).
[9] Y. Kusano, C. Christou, Z. H. Barber, J. E. Evetts, and I. M. Hutchings, Thin Solid Films **355**, 117 (1999).
[10] W. T. Zheng, W. X. Yu, H. B. Li, Y. M. Wang, P. J. Cao, Z. S. Jin, E. Broitman, and J. E. Sundgren, Diamond Relat. Mater. **9**, 1790 (2000).
[11] S. E. Rodil, A. C. Ferrari, J. Robertson, and W. I. Milne, J. Appl. Phys. **89**, 5425 (2001).

[12] D. Li, Y.-W. Chung, S. Yang, M.-S. Wong, F. Adibi, and W. D. Sproul, J. Vac. Sci. Technol. A **12**, 1470 (1994).
[13] J. LaManna, J. Braddock-Wilking, S.-H. Lin, and B. J. Feldman, Solid State Commun. **109**, 573 (1999).
[14] S.-H. Lin, J. Braddock-Wilking, and B. J. Feldman, Solid State Commun. **114**, 193 (2000).
[15] J. C. Sánchez-López, C. Donnet, F. Lefèbvre, C. Fernández-Ramos, and A. Fernández, J. Appl. Phys. **90**, 675 (2001).
[16] E. Broitman, N. Hellgren, O. Wanstrand, M. P. Johansson, T. Berlind, H. Sjöström, J.-E. Sundgren, M. Larsson, and L. Hultman, Wear **248**, 55 (2001).
[17] N. Hellgren, M. P. Johansson, B. Hjörvarsson, E. Broitman, M. Ostblom, B. Liedberg, L. Hultman, and J.-E. Sundgren, J. Vac. Sci. Technol. A **18**, 2349 (2000).
[18] W. J. Gammon, D. I. Malyarenko, O. Kraft, G. L. Hoatson, A. C. Reilly, and B. C. Holloway, Phys. Rev. B **66**, 153402 (2002).
[19] E. O. Stejskal and J. D. Memory, *High Resolution NMR in the Solid State* (Oxford, New York, 1994).
[20] X. Wu and K. W. Zilm, J. Magn. Reson., Ser. A **102**, 205 (1993).
[21] W. C. Oliver and G. M. Pharr, J. Mater. Res. **7**, 1564 (1992).
[22] Y. Ba, H.-M. Kao, C. P. Grey, L. Chopin, and T. Gullion, J. Magn. Reson. **133**, 104 (1998).
[23] Y.-G. Yoon, B. G. Pfrommer, F. Mauri, and S. G. Louie, Phys. Rev. Lett. **80**, 3388 (1998).
[24] G. C. Levy and R. L. Lichter, *Nitrogen-15 Nuclear Magnetic Resonance Spectroscopy* (Wiley, New York, 1979).
[25] T. M. Duncan, *A Compilation of Chemical Shift Anisotropies* (Farragut Press, Chicago, 1990).
[26] Å. Johansson and S. Stafström, J. Chem. Phys. **111**, 3203 (1999).
[27] A. Snis and S. F. Matar, Phys. Rev. B **60**, 10 855 (1999).
[28] H. Sjöström, L. Hultman, J. E. Sundgren, S. V. Hainsworth, T. F. Page, and G. Theunissen, J. Vac. Sci. Technol. A **14**, 56 (1996).